A Godunov-Type Scheme for Nonhydrostatic Atmospheric Flows

Nash'at Ahmad

School of Computational Sciences
George Mason University
March 23rd, 2004

Objective

The objective of this project was to develop a high-resolution flow solver on unstructured mesh for solving the Euler and Navier-Stokes equations governing atmospheric flows

Overview

- Background
- Properties of Euler Equations
- Godunov Scheme
- Harten-Lax-van Leer-Contact (HLLC) approximate Riemann Solver (Toro *et* al.)
- Monotone Upstream Schemes for Conservation Laws (MUSCL)
- Comparison with other schemes
- Implementation on Unstructured Meshes
- Results on Unstructured Meshes
- Conclusions/Future Work

Scales

A Hierarchy of Atmospheric Forcings (from Bacon)

Scenario	Pressure Change (mb)	Horizontal Scale (km)	pressure gradient (mb/km)
Synoptic (meso-α)	10	1000	0.01
Mesoscale (meso-β)	10	100	0.10
Urban Scale – Light Winds (2kt)	0.006	0.05	0.12
Cloud Scale (meso-γ)	2	4	0.50
Land/Sea Boundary	1	1	1.00
Urban Scale – Thermal 2K Heat Island	24	20	1.20
Urban Scale – Strong Winds (10 kt)	0.16	0.05	3.20
Terrain Elevation (5% Grade)	5	1	5.00

Why Unstructured Mesh ?

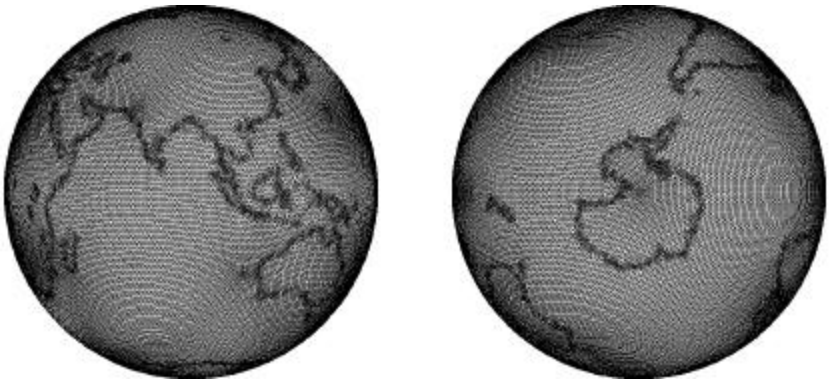

- Provide continuous variable resolution
- Discretize complex geometries
- Solution Adaptation – Efficient use of computational resources

Atmospheric Applications on Unstructured Meshes

- **Scalar Transport**
- Ghorai, *et* al. (Godunov)
- Varvayani, *et* al. (FEM)
- Behrens, *et* al. (Semi-Lagrangian)

- **Navier-Stokes Equations**
- Bacon *et* al. (Smolarkiewicz)

Background – Numerical Scheme

- Central finite difference schemes such as Leapfrog are favored
- Non-conservative discretizations
- Exhibit large amounts of dispersion errors
- Can generate false negatives in important scalars
- Can become unstable in regions of high gradients
- Time filters used to ensure stability often degrade the accuracy of numerical results

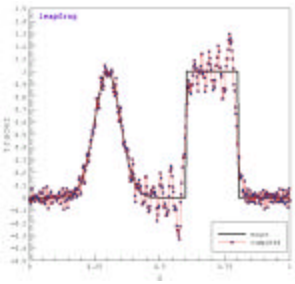

Possible Candidates

- Godunov-type schemes (Godunov, van Leer)
- Flux-Corrected Transport (Boris and Book)
- Central schemes (Jameson, Nessyahu-Tadmor)

Godunov-Type Schemes

- **Hyperbolic Conservation Laws**
- **Characteristics-based Conservative Finite Volume Discretizations**
- **Numerical scheme based on the underlying physics of the equations set**
- **Extensively used in other scientific disciplines:**
  - Löhner, Luo *et* al., Lottati and Eidelman (CFD/Aerodynamics)
  - Wegman (MHD)
  - Ibáñez and Martí (relativistic astrophysics)
  - Vásquez-Cendón (shallow-water equations)
- **Ability to resolve regions of high gradients:**
  - Fronts
  - Drylines
  - Tornados
  - Hurricanes
- **Exhibits minimal phase/dispersion errors**
- **Numerical diffusion can be overcome by higher-order extensions**

Godunov-Type Schemes

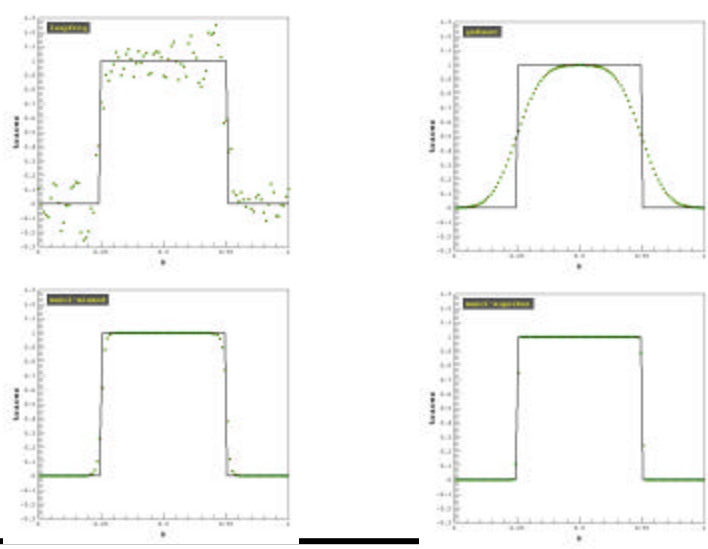

Godunov-Type Schemes for Atmospheric Flow Simulations

- **Scalar Transport**
- Ghorai, *et* al. (Unstructured)
- Hubbard and Nikiforakis (Structured)
- Hourdin and Armengaud (Structured)
- Pietrzak (Structured)

- **Euler Equations**
- Carpenter *et* al. Godunov-PPM (Structured)

Differences from Carpenter *et* al.

- The conservative equation set for modeling compressible flows in the atmosphere is used, in which the conservation of energy is in terms of energy-density ($\rho\theta$) instead of entropy.
- The equations and the solution methodology are in the Eulerian frame of reference rather than Lagrangian.
- An approximate Riemann solver is employed instead of an exact solver to calculate the Godunov fluxes.
- Linear reconstruction of gradients instead of quadratic
- Finally, the scheme is extended to the Navier-Stokes equations (the sub-grid scale diffusion is treated as a source term) and implemented on unstructured meshes.

Navier-Stokes Equations

$$\frac{\partial U}{\partial t}+\frac{\partial F}{\partial x}+\frac{\partial G}{\partial y}=Q+D$$

$$U=\begin{bmatrix} r \\ ru \\ rv \\ rq \end{bmatrix}, \qquad F=\begin{bmatrix} ru \\ ru^2+p \\ ruv \\ ruq \end{bmatrix}, \qquad G=\begin{bmatrix} rv \\ ruv \\ rv^2+p \\ rvq \end{bmatrix}$$

$$p=C_o(rq)^g$$

Using conserved quantities (after Ooyama)

Dry adiabatic atmosphere

The only source term in Q is the gravitational force

Euler Equations (1)

$$\frac{\partial U}{\partial t}+\frac{\partial F}{\partial x}+\frac{\partial G}{\partial y}=0$$

$$U=\begin{bmatrix} r \\ ru \\ rv \\ rq \end{bmatrix}, \qquad F=\begin{bmatrix} ru \\ ru^2+p \\ ruv \\ ruq \end{bmatrix}, \qquad G=\begin{bmatrix} rv \\ ruv \\ rv^2+p \\ rvq \end{bmatrix}$$

$$p=C_o(rq)^g \qquad q=T\left(\frac{p_0}{p}\right)^{\frac{R_d}{c_p}}$$

Euler Equations (2)

$$\frac{\partial U}{\partial t} + \frac{\partial F}{\partial x} = 0$$

$$U = \begin{bmatrix} u_1 \\ u_2 \\ u_3 \end{bmatrix} \equiv \begin{bmatrix} r \\ ru \\ rq \end{bmatrix} \qquad F = \begin{bmatrix} f_1 \\ f_2 \\ f_3 \end{bmatrix} \equiv \begin{bmatrix} ru \\ ru^2 + p \\ ruq \end{bmatrix}$$

Euler Equations (3)

$$U_t + A(U)U_x = 0$$

$$A(U) = \begin{bmatrix} \frac{\partial f_1}{\partial u_1} & \frac{\partial f_1}{\partial u_2} & \frac{\partial f_1}{\partial u_3} \\ \frac{\partial f_2}{\partial u_1} & \frac{\partial f_2}{\partial u_2} & \frac{\partial f_2}{\partial u_3} \\ \frac{\partial f_3}{\partial u_1} & \frac{\partial f_3}{\partial u_2} & \frac{\partial f_3}{\partial u_3} \end{bmatrix}$$

Euler Equations (4)

$$F(U) = \begin{bmatrix} u_2 \\ \dfrac{u_2^2}{u_1} + C_o u_3^g \\ \dfrac{u_2 u_3}{u_1} \end{bmatrix} \quad \Rightarrow A(U) = \begin{bmatrix} 0 & 1 & 0 \\ -u^2 & 2u & a^2/q \\ -uq & q & u \end{bmatrix}$$

$$a = \sqrt{\frac{pg}{r}}$$

Euler Equations (5)

$$\left| A(U) - lI \right| = 0$$

$$l = \begin{bmatrix} u - a \\ u \\ u + a \end{bmatrix}$$

Since, the eigenvalues are real, the system is hyperbolic

Euler Equations (6)

$$AK = lK$$

$$K^1 = \begin{bmatrix} 1 \\ u-a \\ q \end{bmatrix}; \qquad K^2 = \begin{bmatrix} 1 \\ u \\ 0 \end{bmatrix}; \qquad K^3 = \begin{bmatrix} 1 \\ u+a \\ q \end{bmatrix}$$

$$\nabla l_1(U)\cdot K^1 \neq 0; \qquad \nabla l_2(U)\cdot K^2 = 0; \qquad \nabla l_3(U)\cdot K^3 \neq 0$$

- K^2 – *linearly degenerate* – contact
- K^1 and K^3 – *genuinely non-linear* – either shock or rarefaction wave

Godunov's Method and HLLC Riemann Solver

- Godunov's Method
- Monotone Upstream Schemes for Conservation Laws (MUSCL)
- Total Variation Diminishing (TVD) condition – Limiters
- Harten-Lax-van Leer-Contact (HLLC) approximate Riemann Solver
- Comparison with other schemes

Godunov's Method

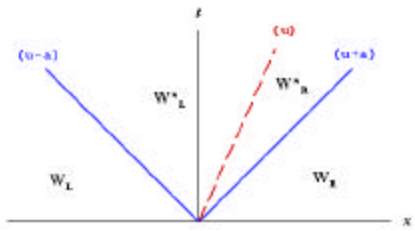

$$U_i^{n+1} = U_i^n + \frac{\Delta t}{\Delta x}\left[F_{i-\frac{1}{2}} + F_{i+\frac{1}{2}}\right]$$

$$F_{i+\frac{1}{2}} = F(U_{i+\frac{1}{2}}(0))$$

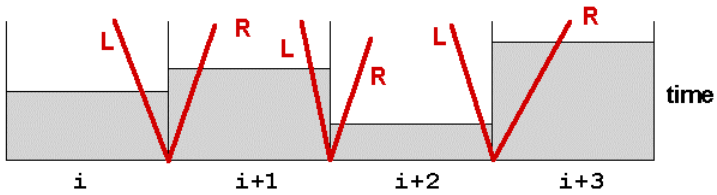

MUSCL (van Leer) – TVD (Harten, Spekreijse)

$$u_{edge} = u_i + f(i)\cdot\nabla u_i \cdot (x_{edge} - x_i)$$

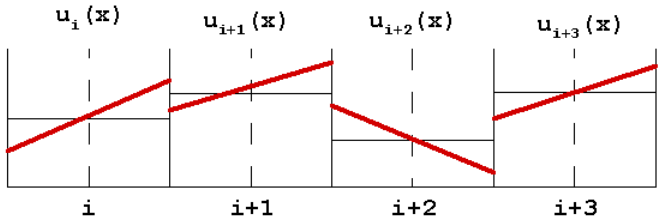

$$\min(u_i, u_{i+1}) \le u_{i+\frac{1}{2}} \le \max(u_i, u_{i+1})$$

- No new local extrema in 'x' may be created
- The value of a local minima increases
- The value of a local maxima decreases

HLLC Riemann Solver (1)

- The approximate Riemann solver Harten-Lax-van Leer-Contact (HLLC) is an extension of the HLL (Harten, Lax, and van Leer) solver by Toro *et* al.
- Ability to resolve contact discontinuities and shear waves
- Positivity preservation of scalar quantities
- Enforcement of the entropy condition

HLLC Riemann Solver (2)

$$F^{HLLC} = \begin{cases} F_L, & if \quad S_L > 0 \\ F_L^*, & if \quad S_L \le 0 < S_* \\ F_R^*, & if \quad S_* \le 0 \le S_R \\ F_R, & if \quad S_R < 0 \end{cases}$$

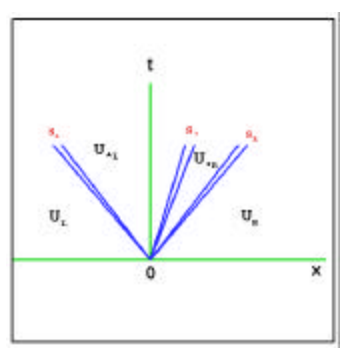

$$F_L \equiv F(U_L) = \begin{pmatrix} (ru)_L \\ (ru^2)_L + p_L \\ (rq)_L \end{pmatrix}, \qquad F_R \equiv F(U_R) = \begin{pmatrix} (ru)_R \\ (ru^2)_R + p_R \\ (rq)_R \end{pmatrix}$$

HLLC Riemann Solver (3)

$$U_t + F(U)_x = 0$$

$$\Delta F = S_i \Delta U$$

$$F_L^* = F_L + S_L\left(U_L^* - U_L\right)$$
$$F_R^* = F_L^* + S_*\left(U_R^* - U_L^*\right)$$
$$F_R^* = F_R + S_R\left(U_R^* - U_R\right)$$

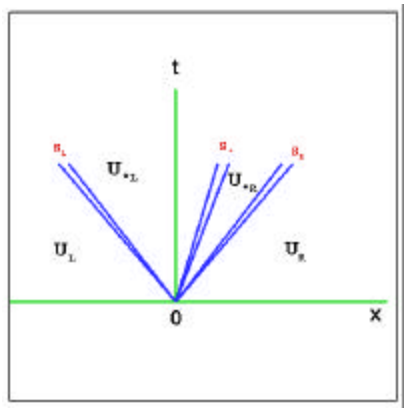

- Three equations four unknowns
- Need to find U^*_L and U^*_R to define F^*_L and F^*_R

HLLC Riemann Solver (4)

Impose the following conditions

$$u_{*L} = u_{*R} = u_* = S_*$$
$$p_{*L} = p_{*R} = p_*$$

HLLC Riemann Solver (5)

$$U_L^* = \begin{pmatrix} r_L^* \\ (ru)_L^* \\ (rq)_L^* \end{pmatrix} = \frac{1}{S_L - S_*} \begin{pmatrix} (S_L - u_L) r_L \\ (S_L - u_L)(ru)_L + (p_L^* - p_L) \\ (S_L - u_L)(rq)_L \end{pmatrix}$$

$$F_L^* \equiv F(U_L^*) = \begin{pmatrix} S_* r_L^* \\ S_*(ru)_L^* + p_L^* \\ S_*(rq)_L^* \end{pmatrix}$$

HLLC Riemann Solver (6)

$$U_R^* = \begin{pmatrix} r_R^* \\ (ru)_R^* \\ (rq)_R^* \end{pmatrix} = \frac{1}{S_R - S_*} \begin{pmatrix} (S_R - u_R) r_R \\ (S_R - u_R)(ru)_R + (p_R^* - p_R) \\ (S_R - u_R)(rq)_R \end{pmatrix}$$

$$F_R^* \equiv F(U_R^*) = \begin{pmatrix} S_* r_R^* \\ S_*(ru)_R^* + p_R^* \\ S_*(rq)_R^* \end{pmatrix}$$

HLLC Riemann Solver (7)

$$S_L = u_L - a_L \qquad S_R = u_R + a_R$$

$$p_L^* = p_L + r_L(S_L - u_L)(S_* - u_L), \qquad p_R^* = p_R + r_R(S_R - u_R)(S_* - u_R)$$

$$S_* = \frac{r_R u_R (S_R - u_R) - r_L u_L (S_L - u_L) + p_L - p_R}{r_R (S_R - u_R) - r_L (S_L - u_L)}$$

Comparison

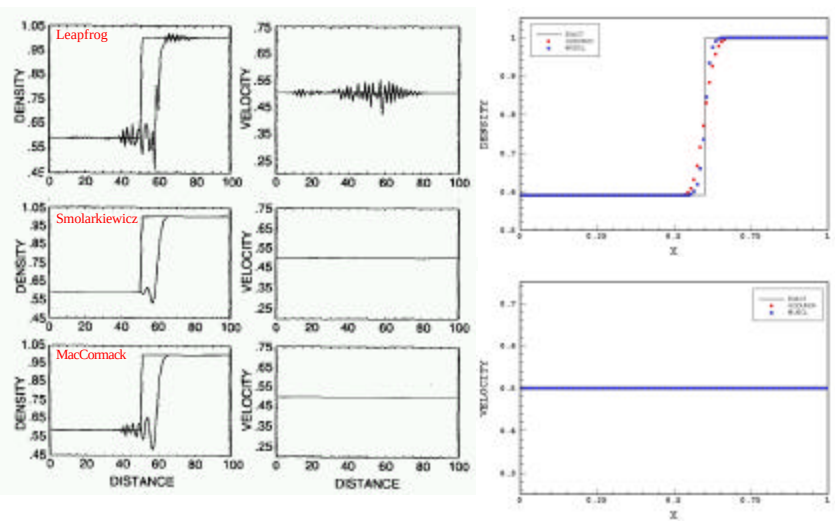

Mendez-Nunez and Caroll, *Mon. Wea. Rev.*, 121, 565-578.

Comparison (cont'd)

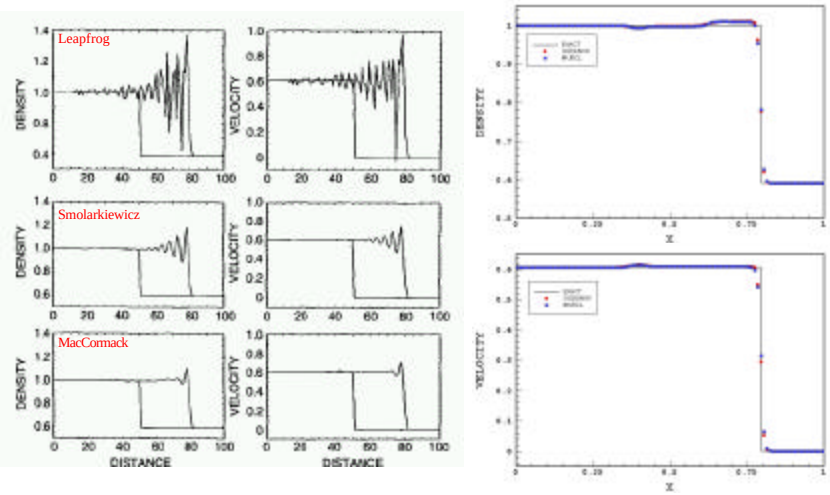

Mendez-Nunez and Caroll, *Mon. Wea. Rev.*, 121, 565-578.

Comparison (cont'd)

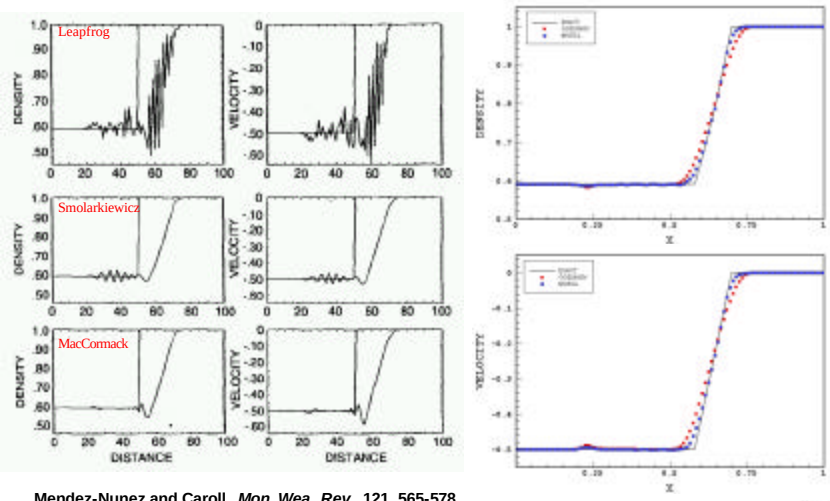

Mendez-Nunez and Caroll, *Mon. Wea. Rev.*, 121, 565-578.

Comparison (cont'd)

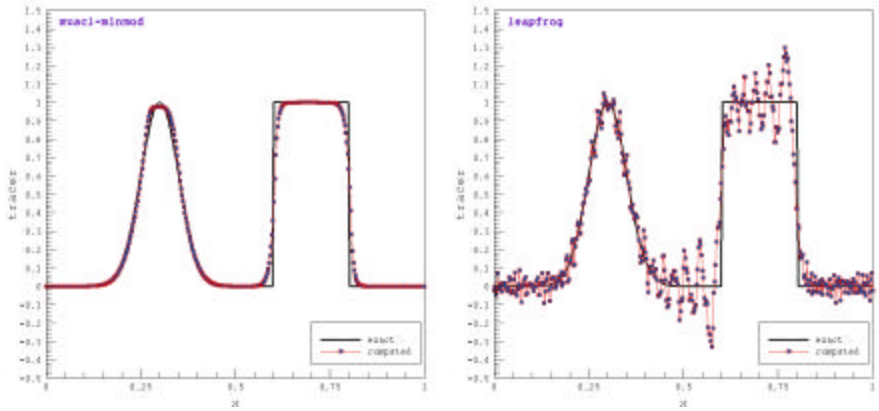

Smagorinsky Scheme

Deformation is related to the eddy viscosity (Smagorinsky-Lilly):

$$K_m = \begin{cases} \dfrac{(c\Delta)^2}{\sqrt{2}} |Def| (1 - Ri)^{0.5} & if \quad Ri < 0.25 \\ 0 & otherwise \end{cases} \qquad Ri = \frac{g}{q} \frac{\dfrac{\partial q}{\partial y}}{\left(\dfrac{\partial u}{\partial y}\right)^2}$$

$$Def^2 = \frac{1}{2} \sum_i \sum_j D_{ij}^2 \qquad Def^2 = \left(\frac{\partial u}{\partial x} - \frac{\partial v}{\partial y}\right)^2 + \left(\frac{\partial u}{\partial y} + \frac{\partial v}{\partial x}\right)^2$$

Runge-Kutta Time Marching

$$U_i^{(0)} = U_i^n$$
$$U_i^{(1)} = U_i^{(0)} - a_1 \Delta t R_i^{(0)}$$
$$U_i^{(2)} = U_i^{(0)} - a_2 \Delta t R_i^{(1)}$$
$$U_i^{(3)} = U_i^{(0)} - a_3 \Delta t R_i^{(2)}$$
$$U_i^{(4)} = U_i^{(0)} - a_4 \Delta t R_i^{(3)}$$
$$U_i^{n+1} = U_i^{(4)}$$

$$\Delta t = CFL \cdot \frac{\Delta x}{abs(u) + a}$$

Implementation on Unstructured Meshes

- Overview
- Data Structures
- Calculation of Convective Fluxes
- Reconstruction
- Limiters
- Boundary Conditions

Implementation on Unstructured Mesh (1)

- OMEGA data structures (Lottati and Eidelman, Bacon *et* al.)
- Higher-order spatial accuracy from either Green-Gauss or Linear-Least Squares reconstruction
- TVD condition enforced *via* slope limiters (Barth-Jesperson or van Leer)
- Limiting performed on conserved variables
- Option of 2 or 4-stage explicit Runge-Kutta Time marching scheme (Jameson-Schmidt-Turkel)
- Diffusion operator calculated using pseudo-Laplacians (Holmes and Connell)
- Subgrid-scale diffusion from Smagorinsky scheme
- Edge-based solver

Implementation on Unstructured Mesh (2)

Cell Connectivity:

```
jelem(cell,1)=iv1 (node1)
jelem(cell,2)=iv2 (node2)
jelem(cell,3)=iv3 (node3)
jelem(cell,4)=ie1 (edge1)
jelem(cell,5)=ie2 (edge2)
jelem(cell,6)=ie3 (edge3)
```

Edge Connectivity:

```
jedge(edge,1)=iv1 (node1)
jedge(edge,2)=iv1 (node2)
jedge(edge,3)=ic1 (cell1)
jedge(edge,4)=ic2 (cell2)
jedge(edge,5)= edge type
```

Cell-centered control volumes

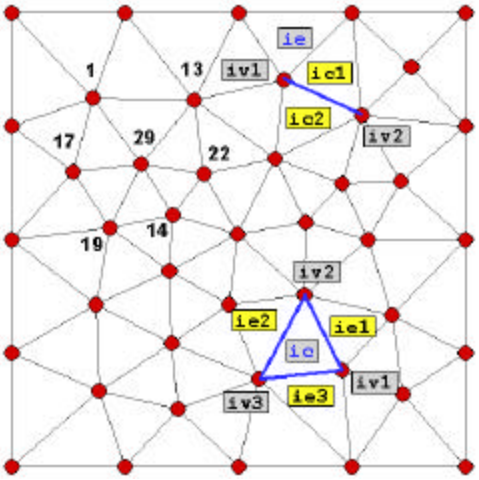

Implementation on Unstructured Mesh (3)

$$\frac{d}{dt}\int_{\Omega} U \; d\Omega = -\oint_{\Gamma} (F,G).\vec{n} \; d\Gamma$$

$$V_{cell}\frac{du_{cell}}{dt} + \sum_{faces}(F,G)\cdot s = 0$$

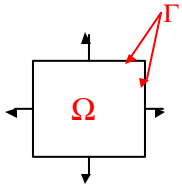

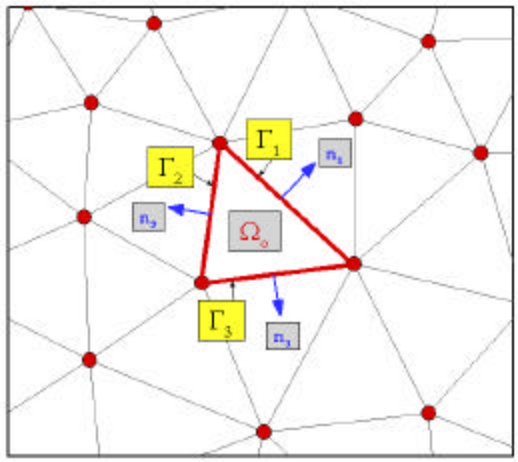

Implementation on Unstructured Mesh (4)

- Reconstruction via either Green-Gauss or Linear Least-Squares
- Option of Barth-Jesperson and van Leer limiters

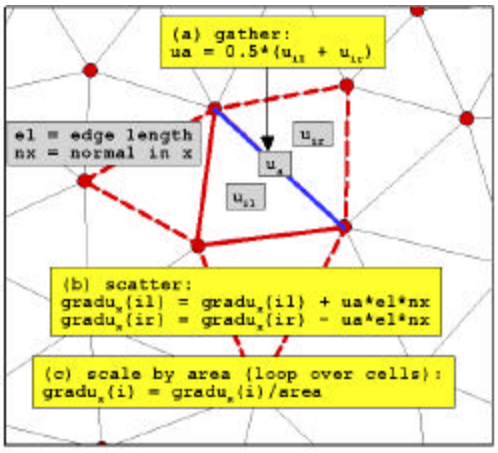

$$u_{edge} = u_i + f(i)\cdot\nabla u_i \cdot (x_{edge} - x_i)$$

$$\int_{\Omega}\nabla u \; d\Omega = \int_{\Gamma} u.\vec{n} \; d\Gamma$$

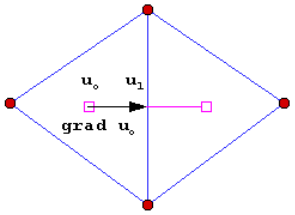

Implementation on Unstructured Mesh (5)

$$u_j^{\min} = \min_{i \in N_j}(\bar{u}_o, \bar{u}_i) \qquad u_j^{\max} = \max_{i \in N_j}(\bar{u}_o, \bar{u}_i)$$

$$u_j^{\min} \leq u(x,y)_o \leq u_j^{\max}$$

$$L_{face} = \begin{cases} \min(1, \dfrac{u_j^{\max} - \bar{u}_o}{u_i^L - \bar{u}_o}) & if \quad u_i^L - \bar{u}_o > 0 \\ \min(1, \dfrac{u_j^{\min} - \bar{u}_o}{u_i^L - \bar{u}_o}) & if \quad u_i^L - \bar{u}_o < 0 \\ 1 & if \quad u_i^L - \bar{u}_o = 0 \end{cases}$$

Scalar Advection Equation

- Rotating Cone Test (convergence)
- Smolarkiewicz's Deformational Flow (stability)
- Doswell's Frontogenesis (accuracy/convergence)
- Solution-Adaptation Demonstration

Rotating Cone Tests

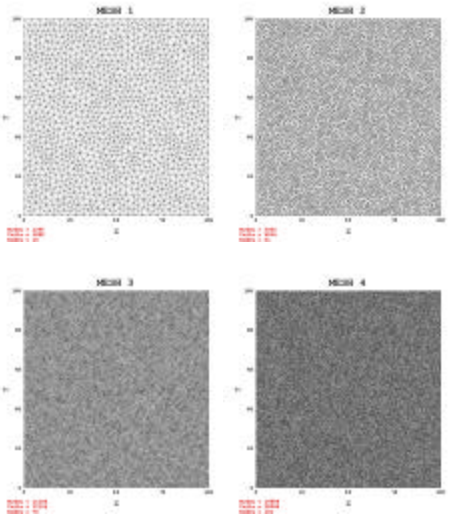

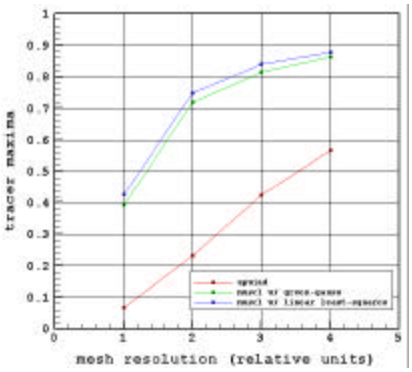

Rotating Cone Tests

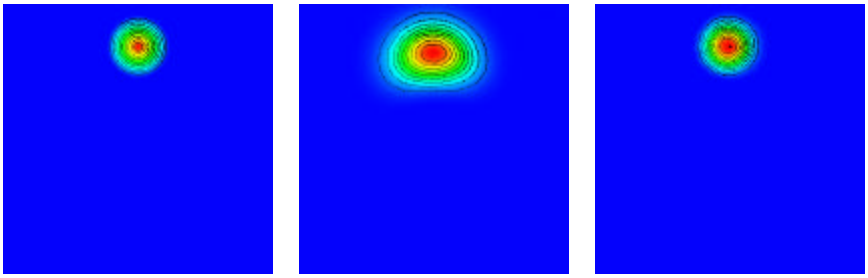

initial condition (left), godunov (center) and muscl (right)

Smolarkiewicz's Deformational Flow

$$u(x,y) = \frac{\partial y}{\partial y} = Ak\sin(kx)\sin(ky)$$

$$v(x,y) = -\frac{\partial y}{\partial x} = Ak\cos(kx)\cos(ky)$$

$$k = \frac{4p}{L}$$

- The flow field consists of sets of symmetrical vortices.
- *A* = 8 and *L* = 100 units (size of the domain was 100x100 units)
- In the words of Smolarkiewicz, "the deformational flow test is a convenient tool for studying a solution's accuracy on the resolved scales and for addressing questions of nonlinear instability due to the existence of unresolved scales"

Smolarkiewicz's Deformational Flow

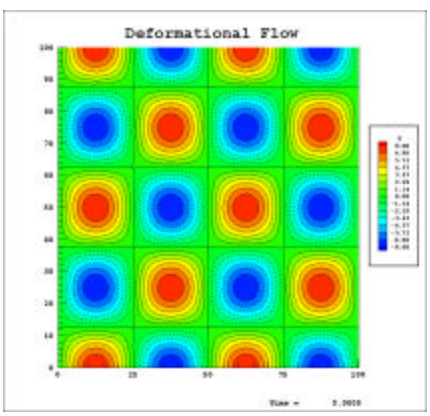

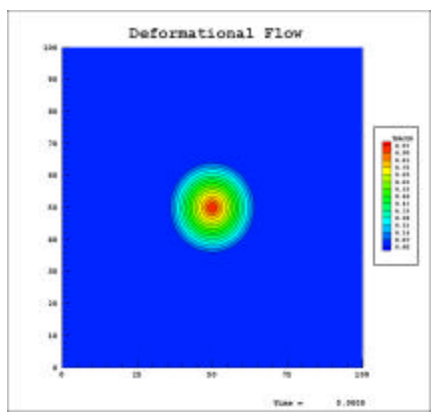

Smolarkiewicz's Deformational Flow

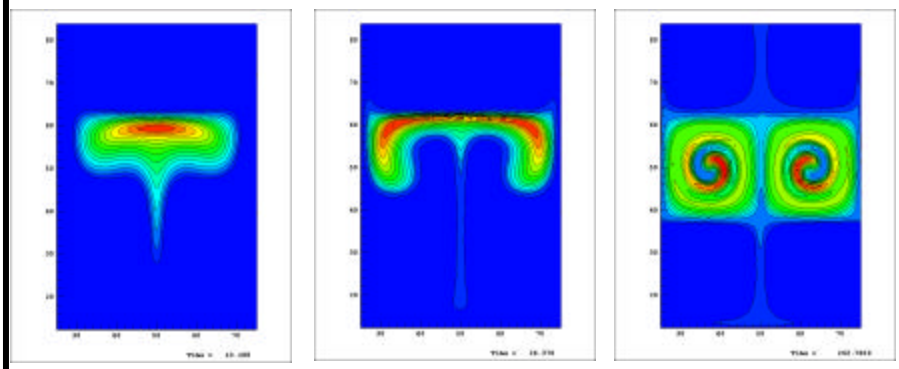

Doswell's Frontogenesis

$$u(x,y) = -\frac{y}{r}\frac{f_t}{f_{\max}}; \quad v(x,y) = \frac{x}{r}\frac{f_t}{f_{\max}} \qquad f_t = \frac{\tanh(r)}{\cosh^2(r)}$$

$$q(x,y,t) = -\tanh\left[\frac{y}{2}\cos(f\cdot t) - \frac{x}{2}\sin(f\cdot t)\right]$$

- Doswell's idealized model describes the interaction of a nondivergent vortex with an initially straight frontal zone
- r is the distance from any given point to the origin of the coordinate system
- f_{max} = 0.385 is the maximum tangential velocity
- The solution domain was bounded within x:[-4,4] and y:[-4,4]
- simulation was run for t = 4 units

Doswell's Frontogenesis

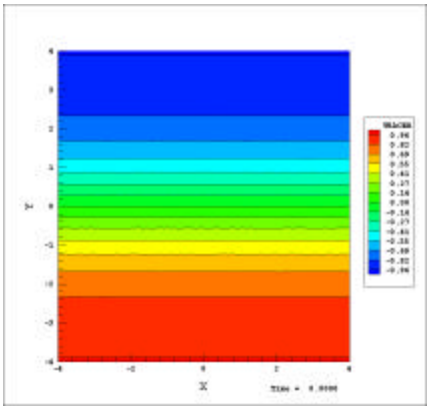

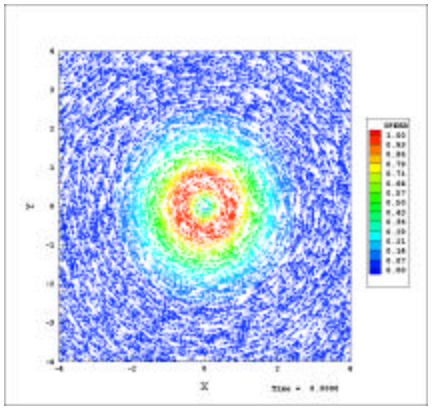

EMC Seminar

Doswell's Frontogenesis

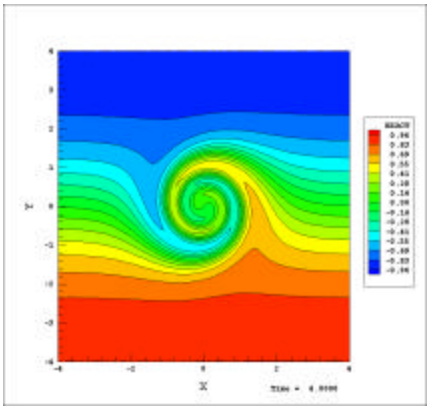

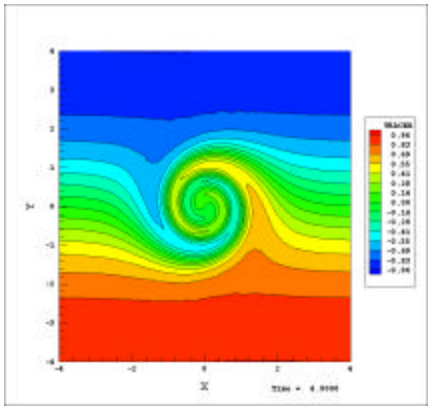

EMC Seminar

Doswell's Frontogenesis

- Three cases:
  - regular mesh (with smoothing)
  - distorted mesh (no smoothing)
  - mesh with right angle triangles
- Comparison of reconstruction techniques
- Accuracy

$$error = \frac{\sqrt{\sum_{1}^{nelem} \left| q_{simulated}(x,y) - q_{exact}(x,y) \right|^2}}{nelem}$$

Doswell's Frontogenesis

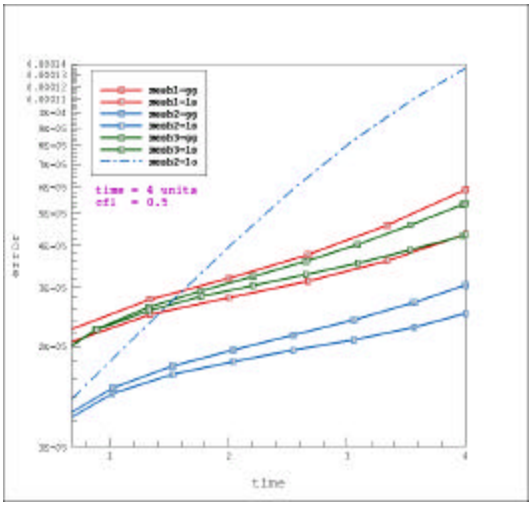

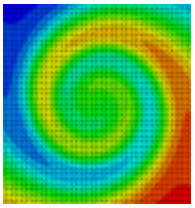

Mesh 1

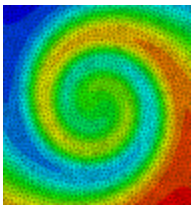

Mesh 2

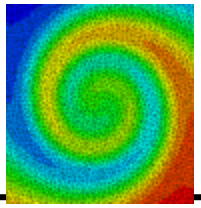

Mesh 3

Convergence and Accuracy

$$\|E\| = C(\Delta x)^s + \textit{higher order terms}$$

$$\log|E| \approx \log|C| + s\log|\Delta x|$$

$$\|E\|_p = \left(\Delta x \sum_{i=-\infty}^{\infty} |E_i|^p\right)^{1/p}$$

EMC Seminar

Doswell's Frontogenesis

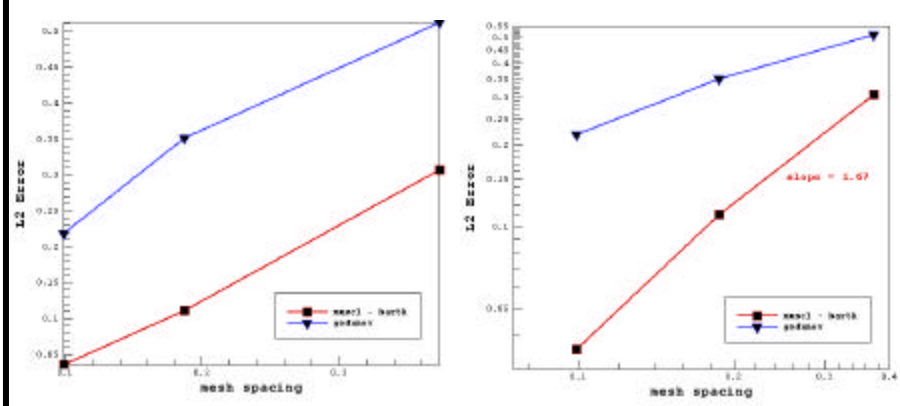

convergence **accuracy**

EMC Seminar

Doswell's Frontogenesis

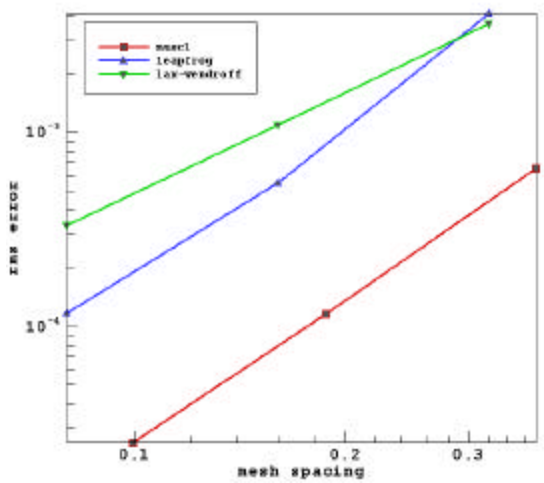

comparison

Dynamic Adaptation

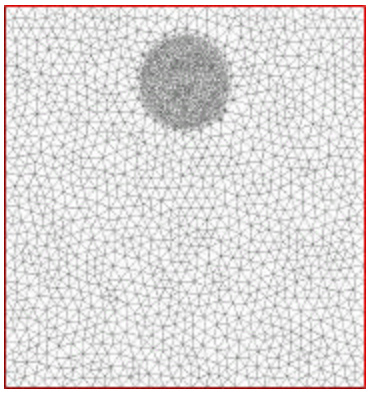

Three Cases:

1. Globally-refined mesh
2. Coarse mesh
3. Adaptive mesh

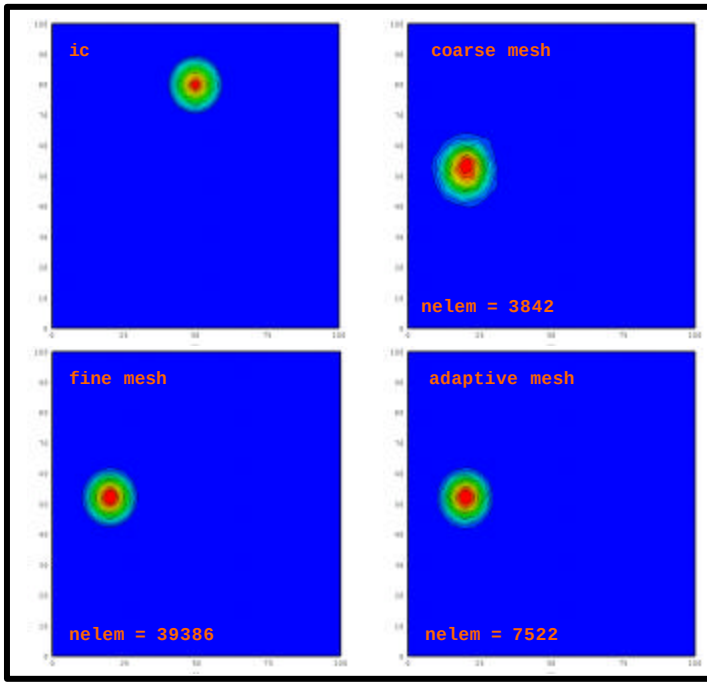

Timings:

Coarse = 01 min
Fine = 29 min
Adapt. = 03 min

EMC Seminar

Dynamic Adaptation

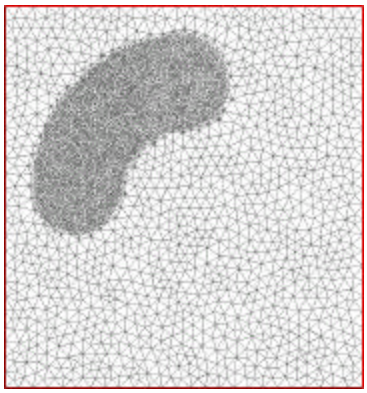

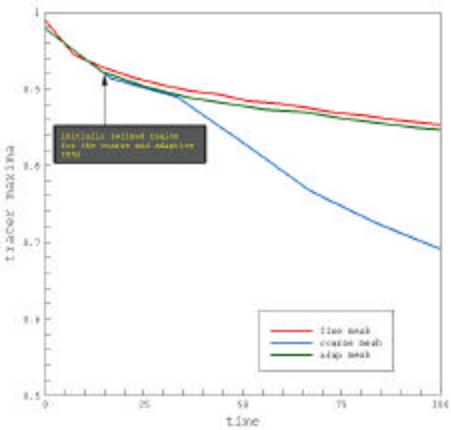

EMC Seminar

Sod Shock Tube

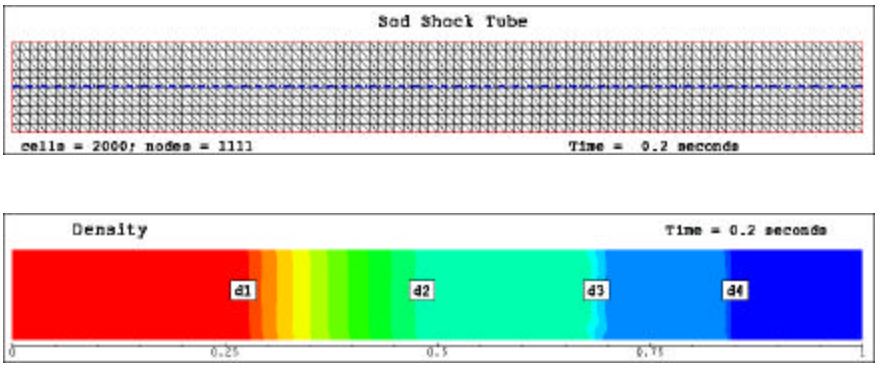

EMC Seminar

Sod Shock Tube

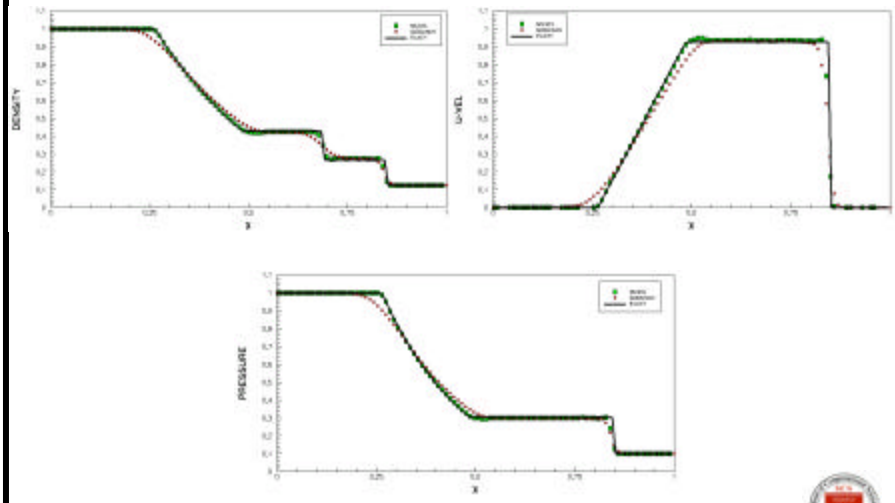

EMC Seminar

Urban Street Canyon

- X [-750 : 750 m]
- Y [0 : 800 m]
- Edge lengths [2.16-12.14 m]
- `nelem = 66585`
- Stable Atmosphere
- Hydrostatic balance initially
- Logarithmic flow profile
- $u_* = 0.2$ m/s
- $y_0 = 15$ cm
- $t_{max} = 21.8$ sec

$$\bar{u}(y) = \frac{u_*}{k} \ln\left(\frac{y}{y_o}\right)$$

Urban Street Canyon

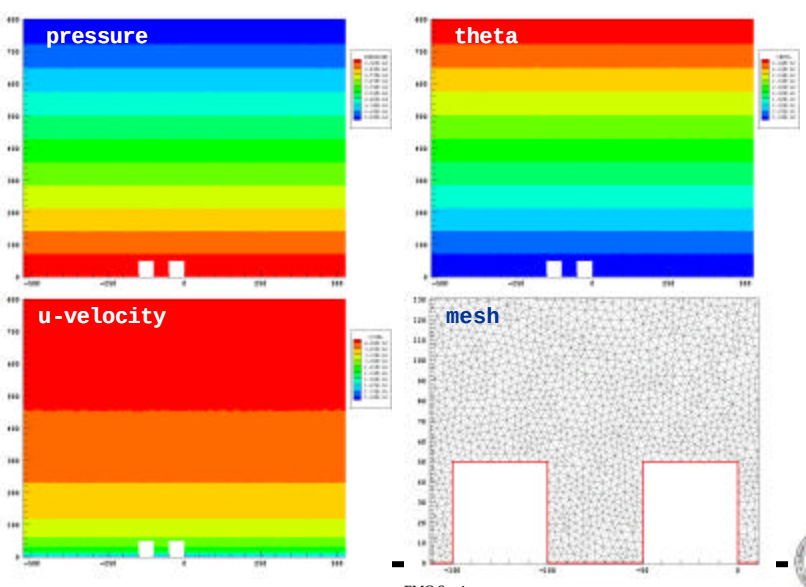

Urban Street Canyon

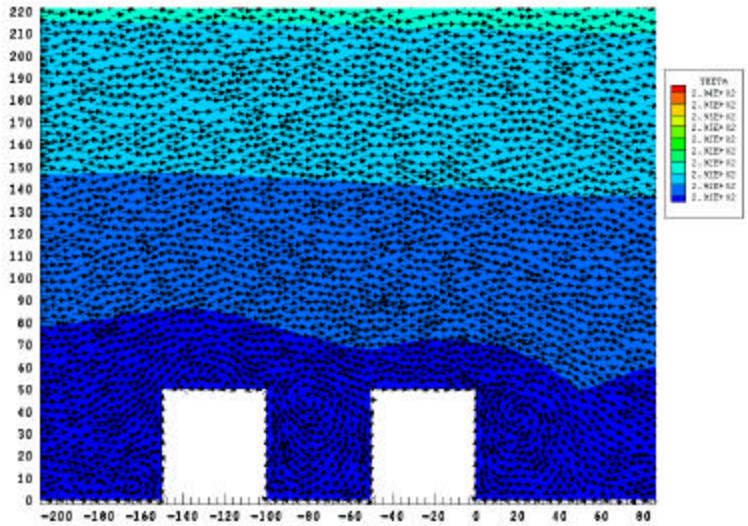

EMC Seminar

Urban Street Canyon

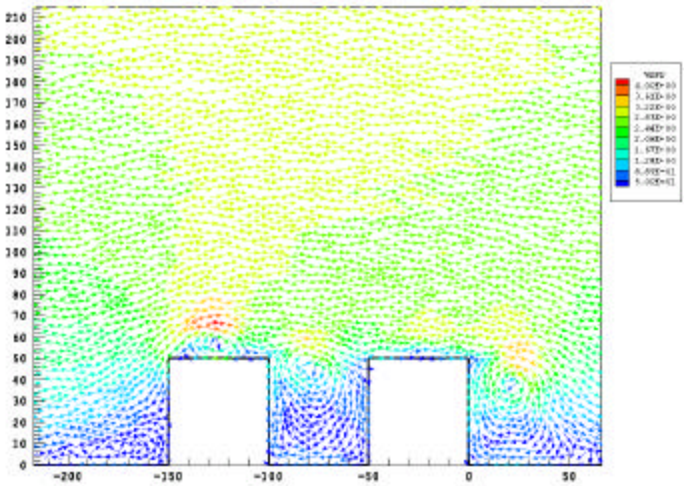

EMC Seminar

Convection in Neutral Atmosphere

- 1km X 1km Domain
- Edge lengths from 3.5m to 12.4m
- Atmosphere at 300K
- Hydrostatic balance initially
- Bubble radius = 100m
- Bubble center height = 120m
- Bubble over-temperature = 6.6K
- Linear temperature profile within the warm bubble
- U = 0 and V = 0
- Fields initialized on a structured grid and then interpolated to the unstructured mesh

Convection in Neutral Atmosphere

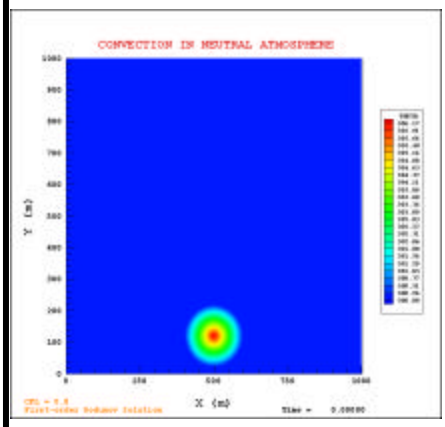

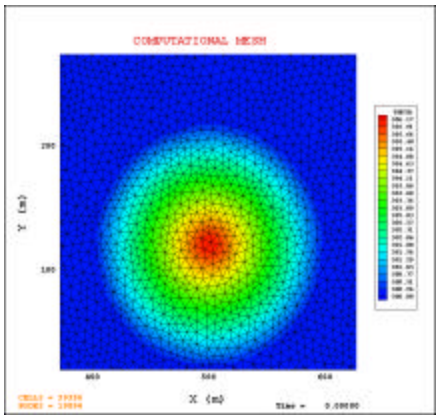

initial conditions

Convection in Neutral Atmosphere

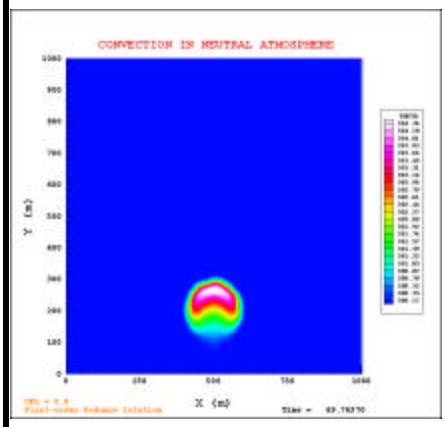

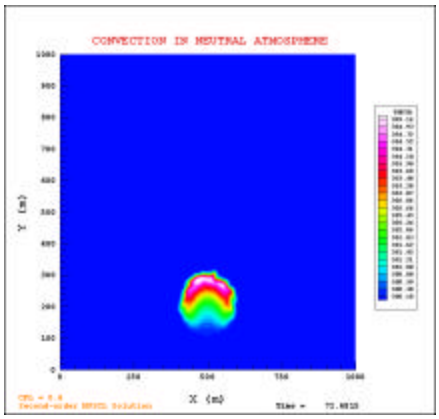

godunov **muscl**

EMC Seminar

Convection in Neutral Atmosphere

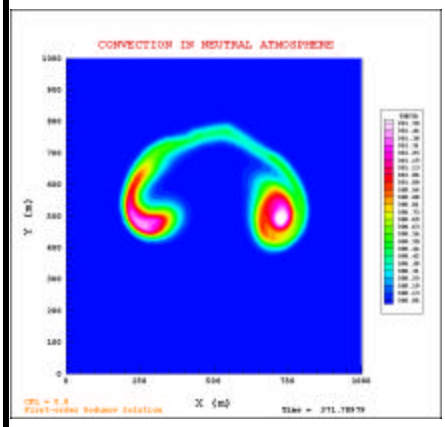

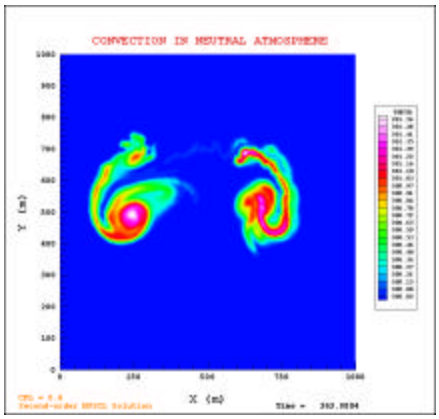

godunov **muscl**

EMC Seminar

Convection in Neutral Atmosphere

godunov **muscl**

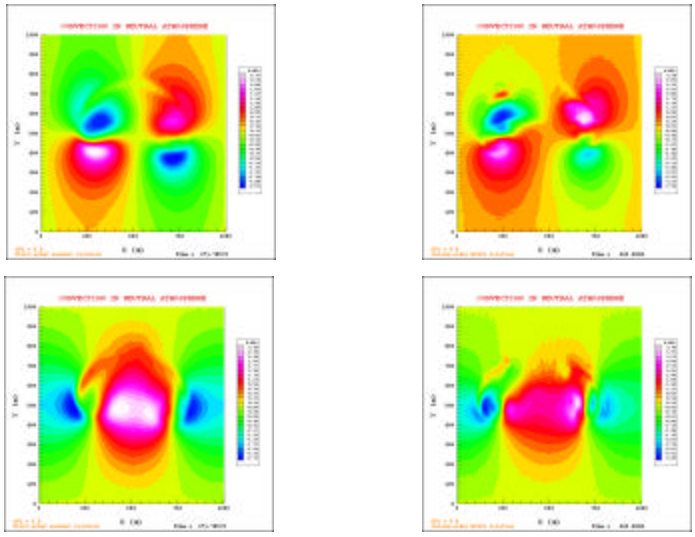

EMC Seminar

Convection in Neutral Atmosphere

Conservation of Mass and Energy-density (Simulation time = 360 s)

Scheme	$E_{initial}$	E_{final}	$M_{initial}$	M_{final}	Iterations
Godunov	334486112	334486112	1114695.5	1114695.6	155,000
MUSCL	334486112	334486114	1114691.6	1114691.7	248,000

EMC Seminar

Kelvin-Helmholtz Instability

Often occurs in the atmosphere.
Sometimes can be observed in billow clouds.
Thought to be a major trigger of clear air turbulence (CAT).

"La Nuit Etoilee"
Vincent van Gogh

$$Ri = \frac{g}{q}\frac{\frac{\partial q}{\partial y}}{\left(\frac{\partial u}{\partial y}\right)^2}$$

Kelvin-Helmholtz Instability

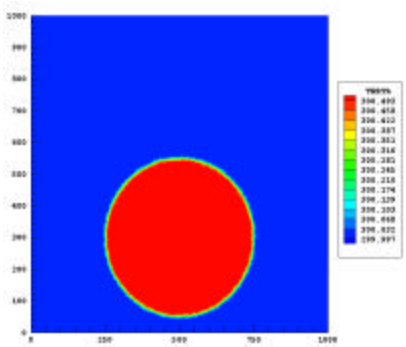

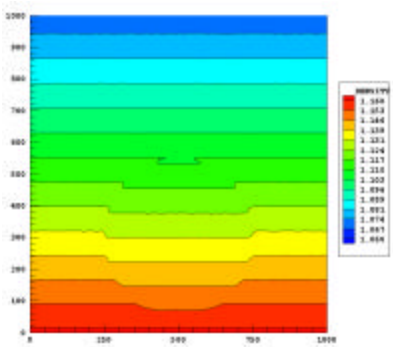

Kelvin-Helmholtz Instability

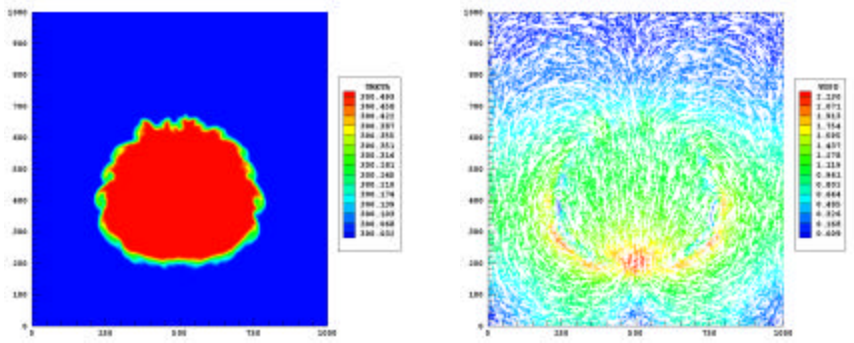

EMC Seminar

Kelvin-Helmholtz Instability

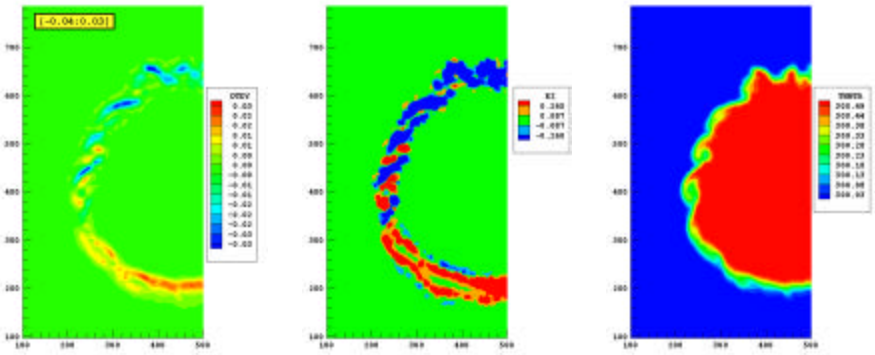

EMC Seminar

Conclusions

- A high-resolution Godunov-type scheme implemented on unstructured meshes for simulating atmospheric flows
- Conservative Finite Volume discretization capable of resolving flows with sharp gradients
- Higher-order spatial accuracy via MUSCL (van Leer)
- Explicit Runge-Kutta time marching
- TVD condition enforced via slope limiters
- Exhibits minimal phase errors and numerical diffusion
- Subgrid-scale diffusion (Smagorinsky closure) added as source term
- Validated against idealized benchmark cases

Future Work

- Implicit time-marching (Sharov, Luo *et* al., Batten *et* al.)
- Examine the role of different types of limiters (Hubbard)
- Extend to three dimensions (prismatic elements)
- Solution-adaptive techniques (Löhner)
- Efficient data structures (Löhner)
- Quadratic reconstruction schemes (Mitchell)
- Test other turbulence schemes (Mellor-Yamada, Germano-Lilly)
- Add more physics (radiation/microphysics)
- Code optimization – Parallelization (MPI)